TITLE

In silico investigation of the binding of MCoTI-II plant defense knottin to the γ-NGF serine protease of the 7S nerve growth factor complex and biological activity of its NGF mimetic properties.

AUTHORS AND AFFILIATION

Peter M. Jones[1], Elizabeth Mazzio[2], Karam Soliman[2] and Anthony M. George[1]*

[1] School of Life Sciences, University of Technology Sydney, P.O. Box 123 Broadway, NSW 2007 Australia

[2] College of Pharmacy and Pharmaceutical Sciences, Florida Agricultural and Mechanical University, 241 Fred Humphries Science Research Facility, Tallahassee, Florida 32307 USA

* To whom correspondence should be addressed:
Phone: +612 9514 4158.
E-mail: tony.george@uts.edu.au

RUNNING TITLE

Binding of the MCoTI-II plant defense knottin to γ-NGF.

KEYWORDS

MCoTI-II; γ-NGF; Plant defense knottin; Nerve growth factor; MD simulations.

CONFLICT OF INTEREST

The authors declare no conflict of interest.

ABSTRACT

Nerve Growth Factor (NGF) induces neurotrophic effects primarily through the tropomyosin-related kinase receptor TrkA NGF. While trophic proteins hold promise for the treatment of neuronal injury and disease, use of NGF is limited by its large molecular weight, lack of permeability through the blood brain barrier and peripheral side effects. High throughput screening on > 1000 natural plant based substances using a PC-12 neurite outgrowth model found only a single NGF mimetic hit, the seed pit of bitter gourd *Momordica cochinchinensis*. Bioactivity guided fractioning of the *M. cochinchinensis* seed extract confirmed the active component to be a protein of approximately 17kD MW, and not of chemical nature. By a theoretical understanding, it has been shown that *in vivo,* NGF exists as an inactive high molecular weight complex known as 7S NGF, which comprises pairs of two serine proteinases α-NGF and γ-NGF, and the trypsin inhibitor β-NGF. Active NGF is comprised of the free β-NGF dimer. Here we use computational modeling, which demonstrates that MCoTI-II can bind stably to the serine protease γ-NGF within the 7S NGF complex. This interaction may inhibit 7S NGF complex formation, potentially freeing the active NFG protein, and may explain the neuritogenic NGF mimetic activity of *M. cochinchinensis* seed extract. Recombinant purified MCoTI-II tested in rat PC-12 cells grown on collagen failed to initiate outgrowth relative to the control. While theoretical dockings studies show a plausible hypothetical explanation for trophic effects, biological studies do not support a role in neurotrophic activity of the pure MCoTI-II protein.

INTRODUCTION

Nerve Growth Factor (NGF) is an endogenously produced polypeptide that promotes the differentiation, survival and repair of neurons in the central and peripheral nervous systems [1-3]. The active form of NGF is a homodimer of two 118 residue polypeptides, of which each contains three intermolecular disulphide bridges in a cystine-knot motif [4, 5]. Its neurotrophic effects are mediated through binding to two types of cell-surface receptors, the tropomyosin-related kinase receptor (Trk) TrkA, and the p75 neurotrophin receptor [6].

In vivo, NGF initially exists as a high molecular weight complex known as 7S NGF [7-11], which comprises the active neurotrophic factor β-NGF dimer (also known as NGF) and two proteinases α-NGF and γ-NGF dimers in the complex (Fig. 1A). The α- and γ-NGF

subunits are closely related Family S1 serine endopeptidases [12], with γ-NGF sharing 37% identity and 69% similarity with bovine trypsin (Fig. S1).

When β-NGF is complexed with 7S NGF, it is inhibited from binding to its cognate receptors and is thus, inactive [13, 14]. Additionally, α-NGF and γ-NGF both competitively block steady-state binding of β-NGF to PC12 cells [15]. These studies indicate that free β-NGF is active and in dynamic equilibrium with the inactive complexed form 7S NGF. Although trophic proteins such as NGF hold promise for the treatment of neuronal injury and disease [16-20], therapeutic applications have been limited by its lack of permeability through the blood brain barrier [21, 22]. In recent years an NGF mimetic has been shown to improve neuronal survival, differentiation, and synaptic plasticity, having relevance for Alzheimer's disease [23], Parkinson's disease [24] and brain / spinal cord injury [25].

Previously, we discovered that an extract of the seed of the *Momordica cochinchinensis* exerted neurotrophic, NGF-mimetic effects in PC-12 cells [26]. While the molecular basis of this effect remains to be determined, the cystine-knot motif of NGF put us in mind of the MCoTI plant defense proteins, which similarly contain a cystine-knot that could bind with high affinity to Family S1 serine endopeptidases [27-29]. MCoTI-I and -II are found in the *M. cochinchinensis* seed and are potent trypsin inhibitors. They are members of the wider Knottin Family of mini-proteins [30, 31], which display exceptional stability due to their unique topology comprising three interlocked disulfide bridges. Knottins have shown great promise as scaffolds for the development of new drugs [32-36].

Notwithstanding the high affinity binding of MCoTI to trypsin, the neurotrophic effect of the seed extract appears unlikely to be mediated via the 7S NGF complex, since it is not present in the extracellular milieu of cultured PC-12 cells. Nevertheless, the above findings led us to consider that if MCoTI-II can bind to α- and/or γ-NGF, such that formation of the 7S NGF complex is affected, the knottin could thereby modulate NGF activity. Of relevance to this idea, Blaber et al (1989) [37] compared the kinetic constants of γ-NGF and bovine pancreatic trypsin for several tripeptide substrates and found that γ-NGF exhibits the higher affinity for most of the substrates examined. Thus, MCoTI-II could have potential as the basis for a drug to modulate NGF levels *in vivo* by freeing β-NGF and allowing for it to have greater activity. To investigate this idea further, molecular modeling

and dynamics simulation were used to analyse the binding of a cyclic knottin trypsin inhibitor to γ-NGF.

RESULTS AND DISCUSSION

The crystal structure of MCoTI-II bound to bovine trypsin [29] was used as a template to dock MCoTI-II to γ-NGF, using the γ-NGF structure from the murine 7S NGF complex [11]. Coordinate alignment showed that 210 of trypsin's 221 Cα atoms aligned with those of γ-NGF with an r.m.s. deviation of 1.02Å, indicating close structural similarity, as expected from the sequence alignment (Fig. S1). The structures differ mostly by the conformation of a number of loops surrounding the active site and the substrate-binding region. They differ significantly only in the region of the kallikrein loop [11], which contains an excision, and is longer in γ-NGF than the corresponding loop is in trypsin (Fig. S1).

Figure 1 illustrates from a structural viewpoint how binding of MCoTI-II to γ-NGF can disrupt formation of the 7S NGF complex. Figure 1A shows the bound inhibitor in the context of the 7S complex, illustrating how it would sit within and prohibit normal interactions between γ-NGF and the C-terminal residues of both protomers of the β-NGF dimer.

Figure 1B (left panel) shows a detailed view of the γ-NGF and β-NGF interaction site. C-terminal residue R118 of β-NGF is bound within the S1 binding pocket of γ-NGF. Experiments have shown that R118 is required for formation of the 7S complex (Moore 1974). Figure 1B (right panel) shows the MCoTI-II docked γ-NGF, illustrating how the inhibitor would interrupt the interaction of γ-NGF with the C-terminal residues of β-NGF. In particular, a lysine residue of MCoTI-II occupies the γ-NGF S1 binding pocket, thereby disallowing the essential interaction between γ-NGF and β-NGF R118. Of note, although γ-NGF was found to exhibit a pronounced preference for substrates with arginine rather than lysine at the P1 position with an order of magnitude difference in K_m, γ-NGF nevertheless bound tripeptide substrates with lysine at P1 with a K_m in the low micromolar range [37].

From this structural alignment, starting coordinates for molecular dynamics simulations of MCoTI-II-bound γ-NGF were generated and a 300 ns simulation run to examine the stability of MCoTI-II bound to γ-NGF. Although the starting coordinates involved a number of steric clashes between ligand and receptor, these were mild enough that they could be relieved by a standard conjugate gradient minimization. This shows that there are no significant steric or structural impediments to the formation of the MCoTI-II-γ-NGF complex.

Figure 2A depicts the time series of the r.m.s deviation of Cα atom coordinates from the initial structure. This shows that the MCoTI-II-bound γ-NGF complex is stable and becomes more so after an initial period where the ligand and receptor adjust to each other. To examine the stability of the ligand-receptor interaction further, Figure 2B depicts the time series of the distance between the geometric centres of MCoTI-II and γ-NGF during the simulation. This shows that the complex evolves toward a closer and less fluctuating interaction across the simulation. For comparison, Figure 2C shows the equivalent distance between MCoTI-II and trypsin from our previously reported simulation [38] that began with a crystal structure of the complex [29]. These data show that the MCoTI-II-γ-NGF complex evolves over 300 ns to an interaction closely similar in respect of its overall ligand-receptor distance to that observed in the simulation of the MCoTI-II-trypsin complex.

Overall the modeling analysis presented here, support the hypothesis that natural knottin serine protease inhibitors within the extract could exert an NGF-mimetic effect by binding to γ-NGF and thereby shift the equilibrium between the active, free β-NGF and the inactive 7S complexed form, toward the active form of the neurotrophic factor.

Given that the seed protein induces neurite outgrowth in the absence of exogenous NGF, we evaluated if a synthetic recombinant protein of the same used in docking (MCoTI-II) could of itself induce NGF mimetic effects in PC-12 cells. The validity of the synthetic peptide sequence and purity (Figures 3A and 3B) were followed by biological studies which failed to show any neurite outgrowth over 7 days in PC-12 cells grown on collagen coated plates (Table 1). In conclusion, further research will be required to both identify the seed protein responsible for inducing neurite outgrowth as well as full annotation of the *M. cochinchinensis* proteome.

METHODS

System Preparation.

The starting coordinates for MD simulations were from the X-ray crystal structures of MCoTI-II bound to bovine trypsin (PDB 4GUX, chains A and D; [29]) and the γ-NGF subunit from the mouse 7S NGF complex (PDB 1SGF, chain G; [11]). To generate initial coordinates of MCoTI-II bound γ-NGF, the γ-NGF subunit was structurally aligned to MCoTI-II bound trypsin using Cα atom coordinates and the 'iterative magic fit' facility in SwissPDBViewer.

The γ-NGF-MCoTI-II complex was solvated in a truncated octahedral periodic cell with a minimum of 20 Å between periodic images, and charge neutralised with a 0.2M NaCl solution. All histidine residues were neutral and protonated at the ε nitrogen, with the exception of the trypsin active site histidine 57, which was neutral and protonated at the δ nitrogen; all other ionisable residues were in the default ionization state.

Simulation parameters

MD simulations were performed using NAMD version 2.11 [39] with the CHARMM27 force field [40], including φ/ψ cross-term map corrections [41], and the TIP3P model for water [42]. The SHAKE and SETTLE algorithms were used to constrain the bonds containing hydrogen to equilibrium length [43]. A cutoff of 12 Å (switching function starting at 10 Å) for van der Waals and real space electrostatic interactions was used. The particle-mesh Ewald method [44] was used to compute long-range electrostatic forces with a grid density of approximately 1/Å3(1/3 Å?). An integration time step of 2 fs was used with a multiple time-stepping algorithm; interactions involving covalent bonds and short-range non-bonded interactions were computed every time-step, while long-range electrostatic forces were computed every two time-steps. Langevin dynamics was utilized to maintain a constant temperature of 310°K with a friction coefficient of 5 ps-1 on all non-hydrogen atoms. A Langevin piston was used to control pressure with a target of 1 atm, a decay period of 100 fs and a damping timescale of 50 fs.

Equilibration and Production Run

The solvated starting structure was minimized using 2000 steps of conjugate gradient minimization without restraints. The minimized structure was then heated from 50°K to 310°K in steps of 25°K using velocity reassignment during a 30 ps MD run. The equilibrated system was used for the production run. The system was run without restraints for 150M integration steps equaling 0.3 μs of real time.

Analysis

VMD [45], Xplor-NIH [46] and Simulaid [47] were used to prepare the system and analyse MD trajectories. All structural figures were prepared using PyMol (http://www.pymol.org/pymol).

Peptide Synthesis and Preparation

The following protein, 1IB9, solution structure of MCOTI-II, from *Momordica cochinchinensis* was sequenced and verified for the recombinant expression construct by Raybio (Norcross, GA, USA). Prior to evaluation *in vitro,* the protein was dissolved in cell culture media at a stock concentration of 1mg/ml.

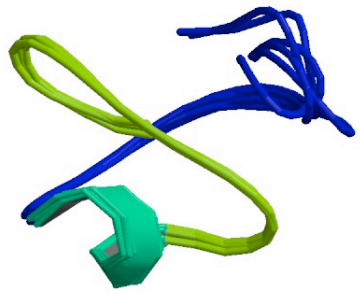

Sequence: SGSDGGVCPK ILKKCRRDSDCPGACICRGNGYCG
Length 34 residues; Mass 3,477 Da.

Cell Viability

Alamar Blue cell viability assay was used to determine the potential cytotoxicity of MCoTI-II. Viable cells reduce a non fluorescent resazurin to resorufin, a fluorescence product. Briefly, 96-well collagen coated plates were seeded with PC-12 cells at a density of 0.5×10^6 cells/mL. Cells were treated with or without MCoTI-II for 7 days at 37°C, 5%

CO_2. Alamar Blue (0.1 mg/mL in HBSS) was added at 15% v/v to each well and the plates were incubated for 6-8 h. Quantitative analysis of dye conversion was measured using a Synergy™ HTX Multi-Mode microplate reader (BioTek, Winooski, VT, USA), at 550 nm/580 nm (excitation/emission).

Neurite Outgrowth

Neurite outgrowth was assessed by visual observation using an Zeiss standard bright field inverted microscope, with samples compared to a reference positive (7SNGF) 0.5 μg/mL vs negative (HBSS) controls.

REFERENCES

1. Levi-Montalcini, R. & Cohen, S. (1956) In Vitro and in Vivo Effects of a Nerve Growth-Stimulating Agent Isolated from Snake Venom, *Proc Natl Acad Sci U S A.* **42**, 695-9.
2. Esmaeili, A., Alifarja, S., Nourbakhsh, N. & Talebi, A. (2014) Messenger RNA Expression Patterns of Neurotrophins during Transdifferentiation of Stem Cells from Human-Exfoliated Deciduous Teeth into Neural-like Cells, *Avicenna J Med Biotechnol.* **6**, 21-6.
3. Bothwell, M. (2014) NGF, BDNF, NT3, and NT4, *Handb Exp Pharmacol.* **220**, 3-15.
4. Angeletti, R. H. & Bradshaw, R. A. (1971) Nerve growth factor from mouse submaxillary gland: amino acid sequence, *Proc Natl Acad Sci U S A.* **68**, 2417-20.
5. McDonald, N. Q., Lapatto, R., Murray-Rust, J., Gunning, J., Wlodawer, A. & Blundell, T. L. (1991) New protein fold revealed by a 2.3-A resolution crystal structure of nerve growth factor, *Nature.* **354**, 411-4.
6. Kaplan, D. R. & Miller, F. D. (1997) Signal transduction by the neurotrophin receptors, *Curr Opin Cell Biol.* **9**, 213-21.
7. Varon, S., Nomura, J. & Shooter, E. M. (1967) Subunit structure of a high-molecular-weight form of the nerve growth factor from mouse submaxillary gland, *Proc Natl Acad Sci U S A.* **57**, 1782-9.
8. Thomas, K. A., Baglan, N. C. & Bradshaw, R. A. (1981) The amino acid sequence of the gamma-subunit of mouse submaxillary gland 7 S nerve growth factor, *J Biol Chem.* **256**, 9156-66.
9. Ullrich, A., Gray, A., Wood, W. I., Hayflick, J. & Seeburg, P. H. (1984) Isolation of a cDNA clone coding for the gamma-subunit of mouse nerve growth factor using a high-stringency selection procedure, *DNA.* **3**, 387-92.
10. Isackson, P. J., Ullrich, A. & Bradshaw, R. A. (1984) Mouse 7S nerve growth factor: complete sequence of a cDNA coding for the alpha-subunit precursor and its relationship to serine proteases, *Biochemistry.* **23**, 5997-6002.
11. Bax, B., Blundell, T. L., Murray-Rust, J. & McDonald, N. Q. (1997) Structure of mouse 7S NGF: a complex of nerve growth factor with four binding proteins, *Structure.* **5**, 1275-85.

12. Ronne, H., Anundi, H., Rask, L. & Peterson, P. A. (1984) 7S Nerve growth factor alpha and gamma subunits are closely related proteins, *Biochemistry.* **23**, 1229-34.
13. Harris-Warrick, R. M., Bothwell, M. A. & Shooter, E. M. (1980) Subunit interactions inhibit the binding of beta nerve growth factor to receptors on embryonic chick sensory neurons, *J Biol Chem.* **255**, 11284-9.
14. Stach, R. W. & Shooter, E. M. (1980) Cross-linked 7S nerve growth factor is biologically inactive, *J Neurochem.* **34**, 1499-505.
15. Woodruff, N. R. & Neet, K. E. (1986) Inhibition of beta nerve growth factor binding to PC12 cells by alpha nerve growth factor and gamma nerve growth factor, *Biochemistry.* **25**, 7967-74.
16. Cui, X., Chen, L., Ren, Y., Ji, Y., Liu, W., Liu, J., Yan, Q., Cheng, L. & Sun, Y. E. (2013) Genetic modification of mesenchymal stem cells in spinal cord injury repair strategies, *Biosci Trends.* **7**, 202-8.
17. Kuihua, Z., Chunyang, W., Cunyi, F. & Xiumei, M. (2014) Aligned SF/P(LLA-CL)-blended nanofibers encapsulating nerve growth factor for peripheral nerve regeneration, *J Biomed Mater Res A.* **102**, 2680-91.
18. Kuo, Y. C. & Wang, C. T. (2014) Protection of SK-N-MC cells against beta-amyloid peptide-induced degeneration using neuron growth factor-loaded liposomes with surface lactoferrin, *Biomaterials.* **35**, 5954-64.
19. Yu, H., Liu, J., Ma, J. & Xiang, L. (2014) Local delivery of controlled released nerve growth factor promotes sciatic nerve regeneration after crush injury, *Neurosci Lett.* **566**, 177-81.
20. Zhang, H., Wu, F., Kong, X., Yang, J., Chen, H., Deng, L., Cheng, Y., Ye, L., Zhu, S., Zhang, X., Wang, Z., Shi, H., Fu, X., Li, X., Xu, H., Lin, L. & Xiao, J. (2014) Nerve growth factor improves functional recovery by inhibiting endoplasmic reticulum stress-induced neuronal apoptosis in rats with spinal cord injury, *J Transl Med.* **12**, 130.
21. Backman, C., Rose, G. M., Hoffer, B. J., Henry, M. A., Bartus, R. T., Friden, P. & Granholm, A. C. (1996) Systemic administration of a nerve growth factor conjugate reverses age-related cognitive dysfunction and prevents cholinergic neuron atrophy, *J Neurosci.* **16**, 5437-42.
22. Poduslo, J. F. & Curran, G. L. (1996) Permeability at the blood-brain and blood-nerve barriers of the neurotrophic factors: NGF, CNTF, NT-3, BDNF, *Brain Res Mol Brain Res.* **36**, 280-6.
23. Povarnina, P. Y., Vorontsova, O. N., Gudasheva, T. A., Ostrovskaya, R. U. & Seredenin, S. B. (2013) Original Nerve Growth Factor Mimetic Dipeptide GK-2 Restores Impaired Cognitive Functions in Rat Models of Alzheimer's Disease, *Acta Naturae.* **5**, 84-91.
24. Antipova, T. A., Gudasheva, T. A. & Seredenin, S. B. (2011) In vitro study of neuroprotective properties of GK-2, a new original nerve growth factor mimetic, *Bull Exp Biol Med.* **150**, 607-9.
25. Povarina, P., Gudasheva, T. A., Vorontsova, O. N., Nikolaev, S. V., Antipova, T. A., Ostrovskaia, R. U. & Seredin, S. B. (2012) [Neuroprotective effects of a dipeptide mimetic on the GK-2 nerve growth factor in model of permanent common carotid artery occlusion in rats], *Eksp Klin Farmakol.* **75**, 15-20.
26. Mazzio, E., Georges, B., McTier, O. & Soliman, K. F. (2015) Neurotrophic Effects of Mu Bie Zi (Momordica cochinchinensis) Seed Elucidated by High-Throughput Screening of Natural Products for NGF Mimetic Effects in PC-12 Cells, *Neurochem Res.* **40**, 2102-12.
27. Hernandez, J. F., Gagnon, J., Chiche, L., Nguyen, T. M., Andrieu, J. P., Heitz, A., Trinh Hong, T., Pham, T. T. & Le Nguyen, D. (2000) Squash trypsin inhibitors from

Momordica cochinchinensis exhibit an atypical macrocyclic structure, *Biochemistry.* **39**, 5722-30.
28. Chiche, L., Heitz, A., Gelly, J. C., Gracy, J., Chau, P. T., Ha, P. T., Hernandez, J. F. & Le-Nguyen, D. (2004) Squash inhibitors: from structural motifs to macrocyclic knottins, *Curr Protein Pept Sci.* **5**, 341-349.
29. Daly, N. L., Thorstholm, L., Greenwood, K. P., King, G. J., Rosengren, K. J., Heras, B., Martin, J. L. & Craik, D. J. (2013) Structural insights into the role of the cyclic backbone in a squash trypsin inhibitor, *J Biol Chem.* **288**, 36141-8.
30. Le Nguyen, D., Heitz, A., Chiche, L., Castro, B., Boigegrain, R. A., Favel, A. & Coletti-Previero, M. A. (1990) Molecular recognition between serine proteases and new bioactive microproteins with a knotted structure, *Biochimie.* **72**, 431-5.
31. Pallaghy, P. K., Nielsen, K. J., Craik, D. J. & Norton, R. S. (1994) A common structural motif incorporating a cystine knot and a triple-stranded beta-sheet in toxic and inhibitory polypeptides, *Protein Sci.* **3**, 1833-9.
32. Werle, M., Schmitz, T., Huang, H. L., Wentzel, A., Kolmar, H. & Bernkop-Schnurch, A. (2006) The potential of cystine-knot microproteins as novel pharmacophoric scaffolds in oral peptide drug delivery, *J Drug Target.* **14**, 137-46.
33. Craik, D. J., Cemazar, M. & Daly, N. L. (2006) The cyclotides and related macrocyclic peptides as scaffolds in drug design, *Curr Opin Drug Discov Devel.* **9**, 251-60.
34. Wang, C. K., Hu, S. H., Martin, J. L., Sjogren, T., Hajdu, J., Bohlin, L., Claeson, P., Goransson, U., Rosengren, K. J., Tang, J., Tan, N. H. & Craik, D. J. (2009) Combined X-ray and NMR analysis of the stability of the cyclotide cystine knot fold that underpins its insecticidal activity and potential use as a drug scaffold, *J Biol Chem.* **284**, 10672-83.
35. Camarero, J. A. (2017) Cyclotides, a versatile ultrastable micro-protein scaffold for biotechnological applications, *Bioorg Med Chem Lett.* **27**, 5089-5099.
36. Chan, L. Y., Craik, D. J. & Daly, N. L. (2016) Dual-targeting anti-angiogenic cyclic peptides as potential drug leads for cancer therapy, *Sci Rep.* **6**, 35347.
37. Blaber, M., Isackson, P. J., Marsters, J. C., Jr., Burnier, J. P. & Bradshaw, R. A. (1989) Substrate specificities of growth factor associated kallikreins of the mouse submandibular gland, *Biochemistry.* **28**, 7813-9.
38. Jones, P. M. & George, A. M. (2016) Computational analysis of the MCoTI-II plant defence knottin reveals a novel intermediate conformation that facilitates trypsin binding, *Sci Rep.* **6**, 23174.
39. Kale, L., Skeel, R., Bhandarkar, M., Brunner, R., Gursoy, A., Krawetz, N., Phillips, J., Shinozaki, A., Varadarajan, K. & Schulten, K. (1999) NAMD2: Greater Scalability for Parallel Molecular Dynamics, *Journal of Computational Physics.* **151**, 283-312.
40. MacKerell, A. D., Bashford, D., Bellott, M., Dunbrack, R. L., Evanseck, J. D., Field, M. J., Fischer, S., Gao, J., Guo, H., Ha, S., Joseph-McCarthy, D., Kuchnir, L., Kuczera, K., Lau, F. T. K., Mattos, C., Michnick, S., Ngo, T., Nguyen, D. T., Prodhom, B., Reiher, W. E., Roux, B., Schlenkrich, M., Smith, J. C., Stote, R., Straub, J., Watanabe, M., Wiorkiewicz-Kuczera, J., Yin, D. & Karplus, M. (1998) All-Atom Empirical Potential for Molecular Modeling and Dynamics Studies of Proteins, *The Journal of Physical Chemistry B.* **102**, 3586-3616.
41. Mackerell, A. D., Jr., Feig, M. & Brooks, C. L., 3rd (2004) Extending the treatment of backbone energetics in protein force fields: limitations of gas-phase quantum mechanics in reproducing protein conformational distributions in molecular dynamics simulations, *J Comput Chem.* **25**, 1400-15.

42. Jorgensen, W. L., Chandrasekhar, J., Madura, J. D., Impey, R. W. & Klein, M. L. (1983) Comparison of simple potential functions for simulating liquid water, *The Journal of Chemical Physics.* **79**, 926-935.
43. Ryckaert, J.-P., Ciccotti, G. & Berendsen, H. J. C. (1977) Numerical integration of the cartesian equations of motion of a system with constraints: molecular dynamics of n-alkanes, *Journal of Computational Physics.* **23**, 327-341.
44. Darden, T., York, D. & Pedersen, L. (1993) Particle mesh Ewald: An N [center-dot] log(N) method for Ewald sums in large systems, *The Journal of Chemical Physics.* **98**, 10089-10092.
45. Humphrey, W., Dalke, A. & Schulten, K. (1996) VMD: visual molecular dynamics, *J Mol Graph.* **14**, 33-8, 27-8.
46. Schwieters, C. D., Kuszewski, J. J., Tjandra, N. & Clore, G. M. (2003) The Xplor-NIH NMR molecular structure determination package, *J Magn Reson.* **160**, 65-73.
47. Mezei, M. (2010) Simulaid: a simulation facilitator and analysis program, *J Comput Chem.* **31**, 2658-68.

FIGURE LEGENDS

Figure 1.

The 7S NGF complex and modelled γ-NGF-MCoTI-II interaction. Crystal structure of mouse 7S NGF complex (PDB 1SGF; [11] shown in ribbon representation. The protomers of the β-NGF homodimer are colored yellow and red, with C terminal residue β-NGF R118 shown in stick form in red (circled). One γ-NGF subunit is coloured green while the other γ-NGF and the two α-NGF subunits are colored pink, and as indicated. MCoTI-II is shown in surface representation in right panels and colored cyan.

Panel A. Binding of MCoTI-II to γ-NGF in the context of the 7S complex. Left: Shows the 7S complex with one β-NGF- γ-NGF interaction site circled. Right: Same view as left, but showing MCoTI-II docked to γ-NGF in relation to the complex.

Panel B. Detailed view of β-NGF- γ-NGF interaction site. Left: Shows how C-terminal residues of β-NGF interact with the γ-NGF active site and substrate-binding region. Right: Same view as left, showing how bound MCoTI-II would sterically hinder the normal β-NGF- γ-NGF interaction.

Figure 2.

Stability of MCoTI-II-γ-NGF complex during 300ns MD simulation. (A) Time series of the r.m.s deviation of Cα atom coordinates from the initial structure, sampled at 100 ps intervals. (B) Time series of the distance between the geometric centres of Cα atoms of MCoTI-II and γ-NGF, sampled at 100ps intervals. (C) Time series of the distance between the geometric centres of Cα atoms of MCoTI-II and trypsin from previous MD simulation [38].

Figure 3.

(A) HPLC confirmation of purified recombinant MCoTI-II protein. (B) MS/MS confirmation of purified recombinant MCoTI-II protein.

Figure 1

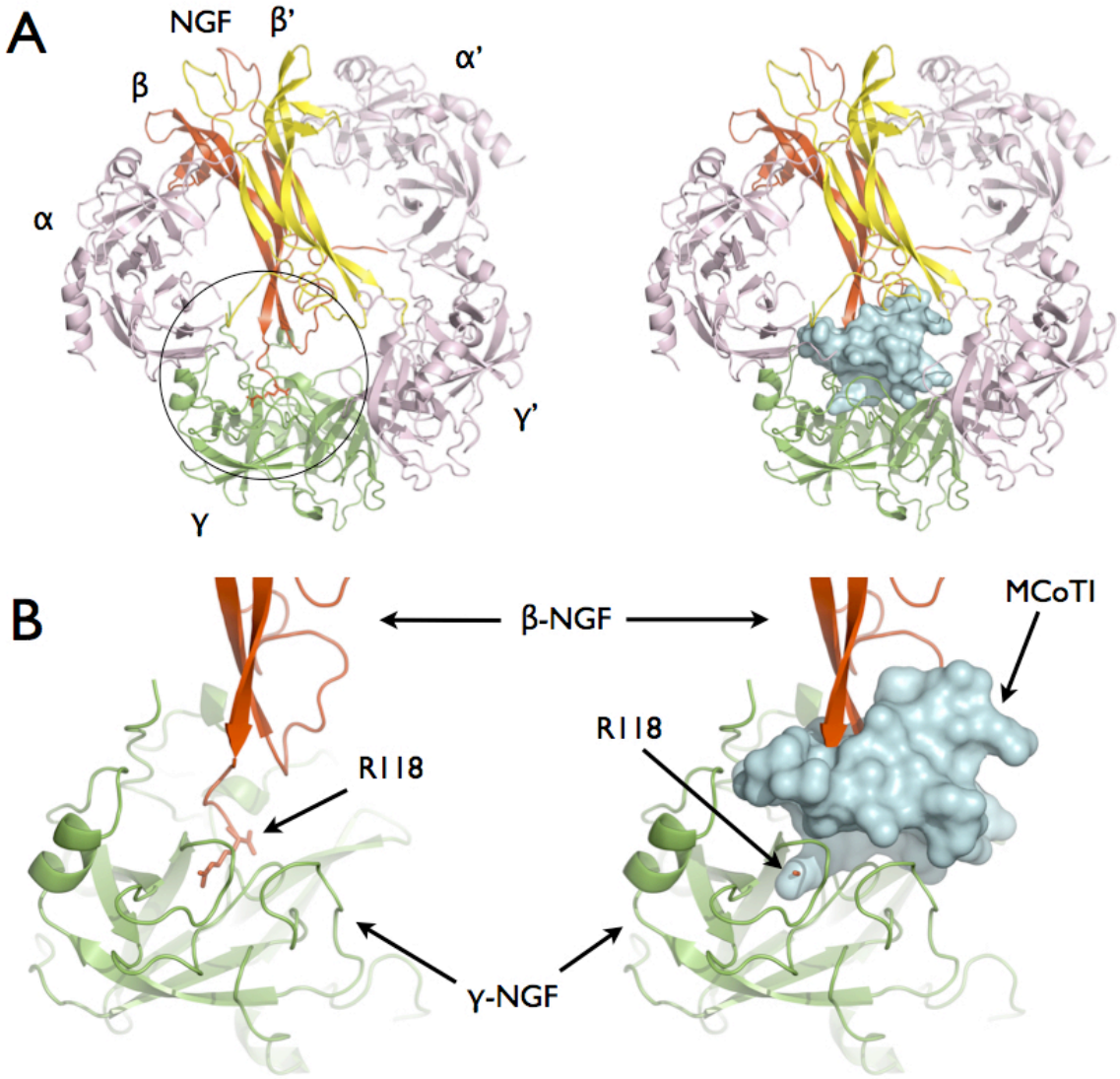

Figure 2

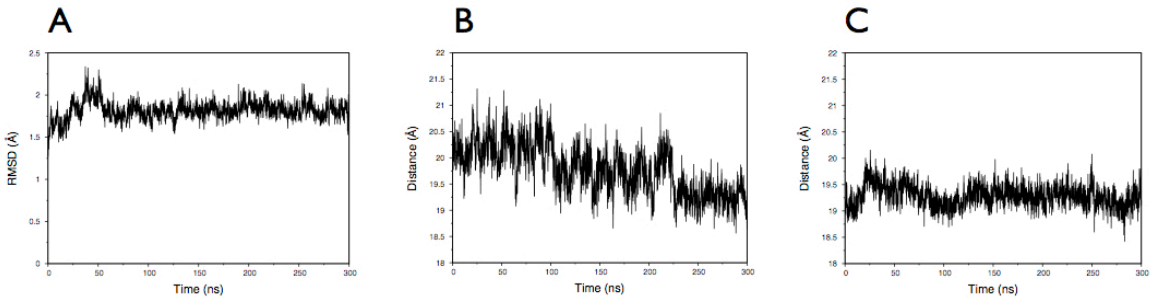

Figure 3A.

Product Name : SG-34
Instrument No. : 03019
Lot No. : P180829-MX675669
Column : 4.6*250mm, Kromasil C18 5um
Solvent A : 0.1% trifluoroacetic in 100% acetonitrile
Solvent B : 0.1% trifluoroacetic in 100% water

Gradient	A	B
0.01min	18%	82%
25.0min	43%	57%
25.1min	100%	0%
30.0min	STOP	

Flow rate : 1.0ml/min
Wavelength : 220nm
Volume : 20ul

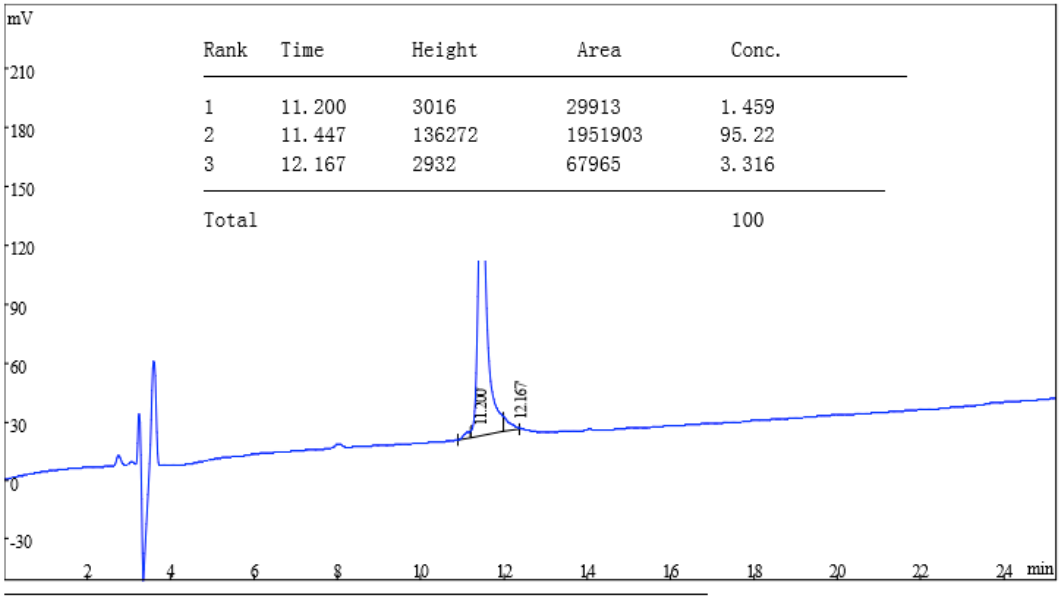

Rank	Time	Height	Area	Conc.
1	11.200	3016	29913	1.459
2	11.447	136272	1951903	95.22
3	12.167	2932	67965	3.316
Total				100

Figure 3A. HPLC confirmation of purified recombinant MCoTI-II protein**.**

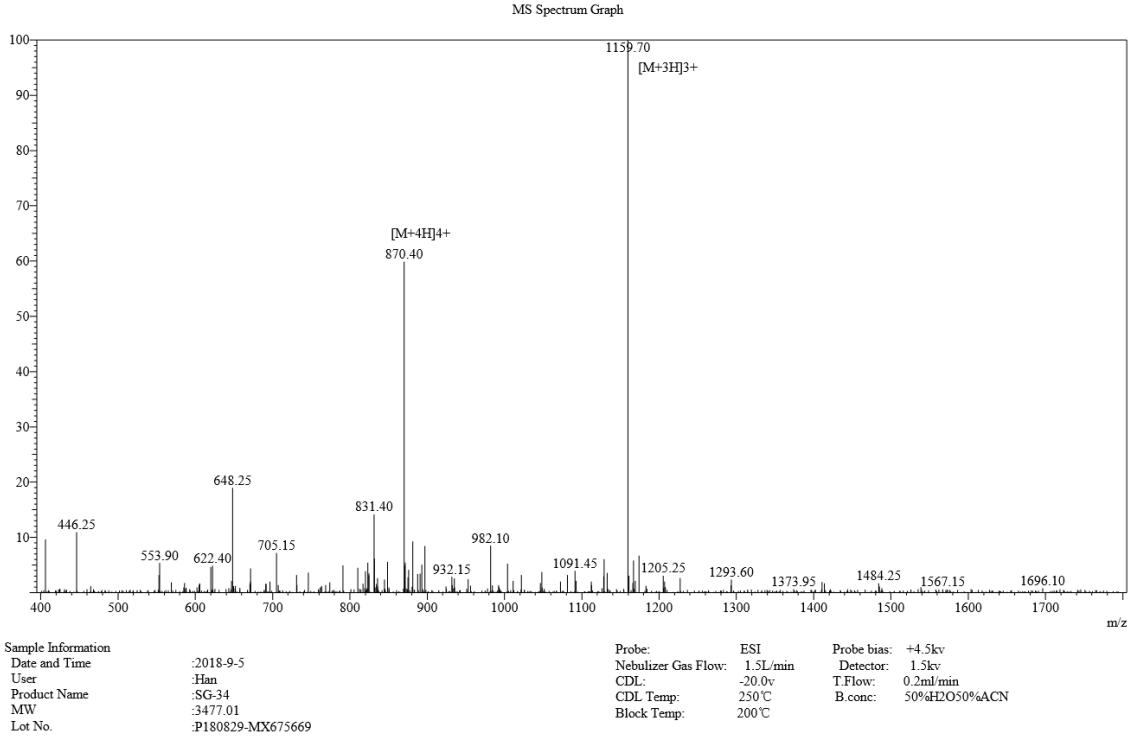

Figure 3B. MS/MS confirmation of purified recombinant MCoTI-II protein.

Table 1.

Table 1: Biological Evaluation		Neurite Outgrowth	Toxicity
Control		-	-
7S-NGF (.5ug/mL)		+	-
MCoTI-II			
175	ug/mL	-	-
157.5	ug/mL	-	-
140	ug/mL	-	-
122.5	ug/mL	-	-
105	ug/mL	-	-
87.5	ug/mL	-	-
70	ug/mL	-	-
52.5	ug/mL	-	-
35	ug/mL	-	-

Table 1. Lack of efficacy for pure recombinant MCoTI-II protein to induce neurite outgrowth in PC-12 cells grown on collagen coated plates for 7 days. The data represents observational analysis for neurite outgrowth and toxicity, relative to negative and positive (NGF -7S from murine submaxillary gland) controls, n=3. There were no significant differences between the control groups and the MCoTI-II groups for neurite outgrowth or cell viability.

Figure S1.

CLUSTAL O (1.2.4) sequence alignment of mouse γ-NGF with bovine trypsin. The N-terminal 24 residues are removed by cleavage at γ-NGF R24 to create the active enzyme. The kallikrein loop in γ-NGF encompasses residues G100 to F112, with residues K108 to R111 being excised in the mature form. With the exception of the kallikrein loop, the sequences of the active enzymes align with only two single-residue gaps, at γ-NGF Y45 and T232.

```
SP|P00760|TRY1_BOVIN  -MKTFIFLALL--GAAVAFPVDDDDKIVGGYTCGANTVPYQVSLNS-GYHFCGGSLINSQ 56
SP|P00756|K1KB3_MOUSE MWFLILFLALSLGGIDAAPPVQ--SRIVGGFKCEKNSQPWHVAVYRYTQYLCGGVLLDPN 58
                           ::****   *   * **   .:*****:.*  *: *::*::     ::*** *:: :
|
SP|P00760|TRY1_BOVIN  WVVSAAHCYKSGIQVRLGEDNINVVEGNEQFISASKSIVHPSYNS-----------NTLN
105
SP|P00756|K1KB3_MOUSE WVLTAAHCYDDNYKVWLGKNNLFKDEPSAQHRFVSKAIPHPGFNMSLMRKHIRFLEYDYS
118
                       **::*****... :* **::*:   * . *.  .**:* **.:*             . .

SP|P00760|TRY1_BOVIN  NDIMLIKLKSAASLNSRVASISLPTSCASAGTQCLISGWGNTKSSGTSYPDVLKCLKAPI
165
SP|P00756|K1KB3_MOUSE NDLMLLRLSKPADITDTVKPITLPTEEPKLGSTCLASGWGSITPTKFQFTDDLYCVNLKL
178
                       **:**::*.. *.:.. *  *:***.  . *: ** ****. . :  .: * * *::  :

SP|P00760|TRY1_BOVIN  LSDSSCKSAYPGQITSNMFCAGYLEGGKDSCQGDSGGPVVCSGKLQGIVSWGS-GCAQKN
224
SP|P00756|K1KB3_MOUSE LPNEDCAKAHIEKVTDAMLCAGEMDGGKDTCKGDSGGPLICDGVLQGITSWGHTPCGEPD
238
                       * :..* .*:  ::*. *:*** ::*****:*:******::*.* ****.***   *.: :

SP|P00760|TRY1_BOVIN  KPGVYTKVCNYVSWIKQTIASN- 246
SP|P00756|K1KB3_MOUSE MPGVYTKLNKFTSWIKDTMAKNP 261
                        ******: ::.****:*:*.*
```